Journal of ELECTRONIC MATERIALS, Vol. 48, No. 9, 2019
https://doi.org/10.1007/s11664-019-07351-y

Thomson Power in the Model of Constant Transport Coefficients for Thermoelectric Elements

JAVIER GARRIDO,[1] ALEJANDRO CASANOVAS,[1] and JOSÉ A. MANZANARES [1,2]

1.—Departamento de Física de la Tierra y Termodinámica, Universitat de València, 46100 Burjassot, Spain. 2.—e-mail: jose.a.manzanares@uv.es

The analytical expressions derived using simple models provide clear insights on the processes in thermoelectric coolers. The model of constant transport coefficients (CTC) considers that the thermal conductivity, the electrical resistivity and the Thomson coefficient are constants. The version of the CTC model that has become standard in the description of the global energy balance may yield grossly inaccurate predictions for thermoelectric cooling applications. We show that these failures can be avoided by accurately describing the Thomson effect in the energy balance. Calculations for bismuth telluride semiconductors show that deviations as large as a factor of three in the Thomson power contribution to the global balance may be found under conditions of practical interest. Compared to the standard version (valid only for moderate temperature gradients), the improved version (valid for highly nonlinear temperature distributions) of the CTC model predicts that a larger fraction of the power released by the electric current leaves the thermoelectric element through the hot boundary. Significant differences in the estimations of the cooling capacity and the coefficient of performance of the thermoelectric cooler are also observed.

Key words: Thermoelectric element, thermoelectric cooling, model of constant transport coefficients, Thomson effect

INTRODUCTION

For some time, the Thomson effect was neglected in the study of thermoelectric elements because of either the difficulties in measuring the Thomson coefficient or its presumed minor importance. In the last decade, it has been recognized that this effect must be taken into account in the energy balance of a thermoelectric module (TEM). Chen et al.[1] suggested that the cooling power of a thermoelectric cooler (TEC) could be improved by a factor of 5–7% due to the Thomson effect. Lee[2] concluded that the assumption of negligible Thomson coefficient could be appropriate for small currents or small temperature differences. Martínez et al.[3] applied finite difference methods and electrical analogies to solve the computational model with temperature-dependent Peltier, Seebeck, Thomson and Joule effects. Wang et al.[4] compared the temperature distributions calculated with and without the Thomson effect. Kanimba et al.[5] developed a one-dimensional (1D) model to take into account temperature-dependent properties of the thermoelectric materials and deduced that the Thomson effect significantly reduces the performance of thermoelectric generators (TEG). Meng et al.[6] developed a three-dimensional model for the TEM taking into account all the thermoelectric effects. Kaushik et al.[7] deduced that the cooling power of a TEC increases up to 10% by the Thomson effect. Manikandan et al.[8] showed that the Thomson effect decreases the maximum power output and efficiency of a TEG. Ruiz-Ortega et al.[9] showed that the Thomson effect increases the cooling power up to 6.5%. Fraisse et al.[10] observed

(Received March 20, 2019; accepted June 4, 2019; published online June 20, 2019)

that the coefficient of performance (COP) of a TEC increases by 17% due to the Thomson effect. Fraisse et al.[11] showed that incorporation of the Thomson effect in the transport model improves the estimation of the COP. Min et al.[12] concluded that the observed decrease in the experimental results of ZT, where Z is the figure of merit and T is the thermodynamic temperature, when the temperature difference increases, can be explained by taking into account the Thomson effect. Arora et al.[13] observed that the Thomson effect significantly reduces various performance parameters of thermoelectric heat pumps. Feng et al.[14] showed that the Thomson effect decreases the cooling capacity by 27% in a TEG-TEC device.

The use of approximate theoretical models is driven by the need of simple equations to analyze the transport processes in TEG and TEC devices.[10,15–17] Ioffe introduced in the 1950s the so-called Ioffe's constant properties approximation, which has become classical since then.[17,18] It considers that the Seebeck coefficient, the thermal conductivity and the electrical resistivity take constant average values. The justification of the model and the choice of the best average values can be based on the comparison with exact results from numerical simulations.[17,19] The name standard simplified model is used[10,15] when the constant values correspond to the mean temperature of the hot and cold sides and the Thomson effect is neglected. The improved simplified model,[10,15] on the contrary, uses a constant Thomson coefficient to take into account the Thomson effect. The latter model introduces the additional assumption that the Thomson power is equitably distributed on both sides of each thermoelectric element (TE),[10–12] which is only valid for small currents and moderate temperature gradients. Another model variation eliminates this additional assumption and hence becomes valid for large currents and highly nonlinear temperature distributions.[20,21] Unfortunately, well-established names for the different model variations are lacking. We refer to the most widespread model,[7–16,18] the one including the additional assumption that the power released by the current leaves the TE symmetrically, as the standard version of the constant transport coefficients (CTC) model. The improved version of the CTC model eliminates this additional assumption.[20,21] The name constant properties model[17] is commonly used for one that neglects the Thomson effect; and, hence, it is avoided here.

The objective of this work is to enhance the understanding of the energy balances in the CTC model. The simplified expressions often used for the heat flows at the TE boundaries (corresponding to the standard CTC model) are critically analyzed on the light of the temperature distribution obtained by integration of the local energy balance. By deriving more accurate expressions of the different contributions in the global energy balance, we aim at highlighting the importance of the Thomson effect.[1–16]

THEORY

The local formulation of the energy conservation under steady-state conditions is (see "Appendix")[22–27]

$$\nabla \cdot (-\kappa \nabla T) - \rho j^2 + \tau \boldsymbol{j} \cdot \nabla T = 0, \tag{1}$$

where κ is the thermal conductivity, ρ is the electrical resistivity, j is the electric current density, $\tau = \mathrm{d}\Pi/\mathrm{d}T - S$ is the Thomson coefficient, S is the Seebeck coefficient, and Π is the Peltier coefficient. Due to the Joule and Thomson effects, the current "releases" energy in the TE. The Thomson contribution $\tau \boldsymbol{j} \cdot \nabla T$ can be positive or negative. Wherever it is positive (negative), the current "absorbs" ("releases") energy due to the Thomson effect.

Many models for thermoelectric elements consider 1D transport using the distance x to the cold junction as the position variable.[2,4–6] Figure 1 schematically shows a thermoelectric cooling device and a thermoelectric generator. The temperature varies from $T(0) = T_\mathrm{c}$ at the cold junction $x = 0$ to $T(\ell) = T_\mathrm{h}$ at the hot junction $x = \ell$. Over a cross-section the temperature is uniform and no lateral "heat losses" are taken into consideration. The x-component of the current density is $j_x = I/A$, where A is the cross-section area. The current is caused by an external power source in the former and by the temperature gradient between a heat source (or burner) and a heat sink in the thermoelectric generator (Fig. 1).[7–16,18,20,21] Heat is absorbed from the surroundings at the cold side of a TEC at a rate $\dot{Q}_\mathrm{c}$ and at the hot side of a TEG at a rate $\dot{Q}_\mathrm{h}$. These rates are related to the Peltier effect at the p-n contact areas, as described below.

The 1D form of the local energy balance is then

$$-A \frac{\mathrm{d}}{\mathrm{d}x}\left(\kappa \frac{\mathrm{d}T}{\mathrm{d}x}\right) - \frac{\rho I^2}{A} + \tau I \frac{\mathrm{d}T}{\mathrm{d}x} = 0. \tag{2}$$

The CTC model considers that κ, ρ and τ are constants with values corresponding to the mean

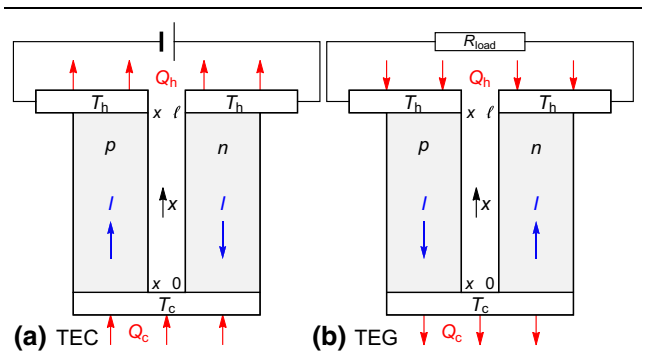

Fig. 1. Thermoelectric cooling device (a) TEC and thermoelectric generator (b) TEG.

temperature $T_m = (T_c + T_h)/2$; hence, the Seebeck coefficient is not constant. This model can be and has been used in TEG and TEC modes. The integration of Eq. 2 over the TE can be presented as $\dot{Q} = \dot{W}$, where $\dot{W} = I^2R - \tau I\Delta T$ is the power released by the current in the TE, $R = \rho l/A$ is the electrical resistance, and $\dot{Q} = -\kappa A[(dT/dx)_h - (dT/dx)_c]$ is the rate of heat transport by thermal conduction out of the TE through its boundaries, $x = 0$ and $x = \ell$. Thus, for fixed T_m, the electric current I and $\Delta T = T_h - T_c$ determine the Joule and Thomson powers, I^2R and $-\tau I\Delta T$.

In the standard CTC model, the power $\dot{W}$ is further assumed to leave the TE symmetrically, that is, half of it through the cold boundary and the other half through the hot boundary,[7–16,18]

$$-\kappa A\left(\frac{dT}{dx}\right)_c \approx -K\Delta T - \frac{1}{2}I^2R + \tau I(T_m - T_c) = -K\Delta T - \frac{\dot{W}}{2}, \quad (3)$$

$$-\kappa A\left(\frac{dT}{dx}\right)_h \approx -K\Delta T + \frac{1}{2}I^2R - \tau I(T_h - T_m) = -K\Delta T + \frac{\dot{W}}{2}, \quad (4)$$

where $K = \kappa A/\ell$ is the thermal conductance. This assumption, however, can only be justified when the current is small and the temperature distribution is almost linear. Note that $T_m - T_c = T_h - T_m = \Delta T/2$.

The improved version of the CTC model eliminates the latter assumption and accurately evaluates the Thomson powers from the nonlinear temperature distribution[16,18,20,21]

$$T(x) = T_c + \Delta T\frac{x}{\ell} + \frac{\dot{W}}{\tau I}\left(\frac{x}{\ell} - \frac{\exp(\tau Ix/K\ell) - 1}{\exp(\tau I/K) - 1}\right) \quad (5)$$

obtained by integration of Eq. 2 with constant κ, ρ and τ. The accurate expressions for the conduction heat flows at the boundaries $x = 0$ and $x = \ell$ are

$$-\kappa A\left(\frac{dT}{dx}\right)_c = -K\Delta T - \frac{1}{2}I^2R + \tau I(\bar{T} - T_c) = -K\Delta T - \frac{\dot{W}}{2}\left[1 - L\left(\frac{\tau I}{2K}\right)\right], \quad (6)$$

$$-\kappa A\left(\frac{dT}{dx}\right)_h = -K\Delta T + \frac{1}{2}I^2R - \tau I(T_h - \bar{T}) = -K\Delta T + \frac{\dot{W}}{2}\left[1 + L\left(\frac{\tau I}{2K}\right)\right], \quad (7)$$

where $L(x) = \coth(x) - 1/x$ is the Langevin function; within 1% accuracy, $L(x) \approx x/3$ for $x < 1/3$. Thus, a fraction $1/2 + L(\tau I/2K)/2$ of the power $\dot{W} = I^2R - \tau I\Delta T$ released by the current leaves the TE through the hot boundary, while a smaller fraction $1/2 - L(\tau I/2K)/2$ leaves the TE through the cold boundary.

The contributions of the Thomson powers are $\tau I(\bar{T} - T_c)$ and $-\tau I(T_h - \bar{T})$. Their approximation in the standard CTC model by the terms $\tau I(T_m - T_c)$ and $-\tau I(T_h - T_m)$ in Eqs. 3 and 4 that can lead to gross errors because the temperature distribution in a TEC is highly nonlinear even for moderate electric currents and, therefore, the average temperature

$$\bar{T} = \frac{1}{\ell}\int_0^\ell T dx = T_m + \frac{\dot{W}}{2\tau I}L\left(\frac{\tau I}{2K}\right) \quad (8)$$

can be significantly different from the mean temperature of the hot and cold junctions, $T_m = (T_c + T_h)/2$. Strictly, $\bar{T} = T_m$ only holds when the current vanishes. In agreement with the physics of the phenomenon, through R and K, the average temperature depends on the sample length ℓ. In particular, $\bar{T} - T_m \approx [\rho(I/A)^2\ell^2 - \tau(I/A)\Delta T\ell]/(12\kappa)$.

The cooling capacity of a TEC is[1,2,11,19,28–36]

$$\dot{Q}_c = \left(\Pi_p - \Pi_n\right)_c I - (1/2)I^2R_{cont} - A\kappa_p\left(\frac{dT_p}{dx}\right)_{x=0} - A\kappa_n\left(\frac{dT_n}{dx}\right)_{x=0} \quad (9)$$

and its coefficient of performance is $COP = \dot{Q}_c/(\dot{Q}_h - \dot{Q}_c)$ with

$$\dot{Q}_h = \left(\Pi_p - \Pi_n\right)_h I + (1/2)I^2R_{cont} - A\kappa_p\left(\frac{dT_p}{dx}\right)_{x=\ell} - A\kappa_n\left(\frac{dT_n}{dx}\right)_{x=\ell}. \quad (10)$$

Here, $(1/2)I^2R_{cont} - (\Pi_p - \Pi_n)_cI$ and $(1/2)I^2R_{cont} + (\Pi_p - \Pi_n)_hI$ are the powers released by the current into the cold ($x = 0$) and hot ($x = \ell$) connectors, respectively; R_{cont} is the resistance of the copper connectors, mainly due to the contact resistance at the copper/semiconductor junctions.

The absence of the Langevin functions in Eqs. 3 and 4 amounts to assuming that the power released by the current in the volume of the TE is driven out of the TE in equal shares through the cold and hot boundaries. This assumption is only justified for TEG applications, when the current is small and the temperature distribution is almost linear. For TEC applications, Eqs. 6 and 7 represent a significant improvement with respect to the standard CTC model[7–16,18] because they accurately describe the importance of the Thomson effect and, hence, they also allow for a more accurate evaluation of the cooling capacity and the COP.

RESULTS AND DISCUSSION

We consider a thermocouple[4,6,37] formed by n-type $Bi_2(Te_{0.94}Se_{0.06})_3$ and p-type $(Bi_{0.25}Sb_{0.75})_2Te_3$ with cross-sectional area $A = 0.50 \times 0.50$ mm^2 and length $\ell = 1.00$ mm. The temperature dependence of the Seebeck coefficients of these materials has been measured by Yamashita,[37] so that the Thomson coefficient can be calculated from the Kelvin relation $\tau = T(dS/dT)$. When the boundary temperatures are $T_h = 320$ K and $T_c = 260$ K, the transport coefficients at $T_m = (T_h + T_c)/2 = 290$ K are[4,6,37] $\kappa_n = 1.662$ W m^{-1} K^{-1}, $\kappa_p = 1.493$ W m^{-1} K^{-1}, $\rho_n = 7.854$ $\mu\Omega$ m, $\rho_p = 8.315$ $\mu\Omega$ m, $\tau_n = -42.36$ μV K^{-1} and $\tau_p = 103.2$ μV K^{-1}. We also use the Kelvin relation $\Pi_p - \Pi_n = (S_p - S_n)T$ with $(S_p - S_n)_c = 422.2$ μV K^{-1} and $(S_p - S_n)_h = 452.4$ μV K^{-1}.[4,6,37]

In the TEC mode, positive values of the COP determine the operational range of electric current, $0 < I \leq 3.0$ A. Figure 2a shows calculations using two values of the contact resistance, $R_{cont} = 0$ and $R_{cont} = 6.5$ mΩ, ca. 10% of the semiconductors electrical resistance.[3,7,38,39] In the TEG mode, the positive values of the electric power

$$P_{out} = (\Pi_p - \Pi_n)_h I - (\Pi_p - \Pi_n)_c I - I^2(R_n + R_p + R_{cont}) + (\tau_n - \tau_p) I \Delta T, \quad (11)$$

where R_n and R_p are the semiconductor electric resistances, determine the operational range of electric current as $0 < I \leq 0.4$ A (Fig. 2b).

In the following we consider the TEC mode. The component I of the electric current in the direction of increasing x is positive in the p-type and negative in the n-type leg (Fig. 1a). The temperature distribution and, hence, the average temperature $\bar{T}$ vary significantly with the current (Fig. 3). In the standard CTC model,[7–16,18] the Thomson powers at the boundaries are approximated by the terms $\tau I(T_m - T_c) = \tau I \Delta T/2$ and $-\tau I(T_h - T_m) = -\tau I \Delta T/2$ in Eqs. 3 and 4, where $T_m = (T_c + T_h)/2$. In the improved CTC model, the Thomson powers are accurately evaluated as $\tau I(\bar{T} - T_c)$ and $-\tau I(T_h - \bar{T})$. The approximation $\tau I \Delta T/2$ underestimates the Thomson power $\tau I(\bar{T} - T_c)$ at the cold junction, by the same amount that $-\tau I \Delta T/2$ overestimates the Thomson power $-\tau I(T_h - \bar{T})$ at the hot junction. The error in the estimation of these Thomson powers is

$$\delta = \delta_{x=0} = \frac{\tau I(\bar{T} - T_c) - \tau I(T_m - T_c)}{\tau I(T_m - T_c)} = -\delta_{x=\ell} = \left(\frac{I^2 R}{\tau I \Delta T} - 1\right) L\left(\frac{\tau I}{2K}\right). \quad (12)$$

Since $\delta = 2(\bar{T} - T_m)/\Delta T$, Fig. 3 also illustrates the importance of these errors. For a current $I = 1.0$ A close to the maximum COP of the TEC, they are $\delta_n = 19\%$ and $\delta_p = 20\%$, and for $I = 1.5$ A they are $\delta_n = 45\%$ and $\delta_p = 49\%$.

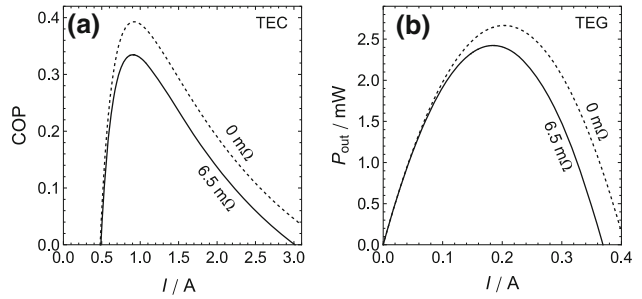

Fig. 2. COP of a TEC (a) and power provided by a TEG (b) made of n-type $Bi_2(Te_{0.94}Se_{0.06})_3$ and p-type $(Bi_{0.25}Sb_{0.75})_2Te_3$, calculated using the improved CTC model, Eqs. 6–11, for two values of the contact resistance, 0 mΩ and 6.5 mΩ.

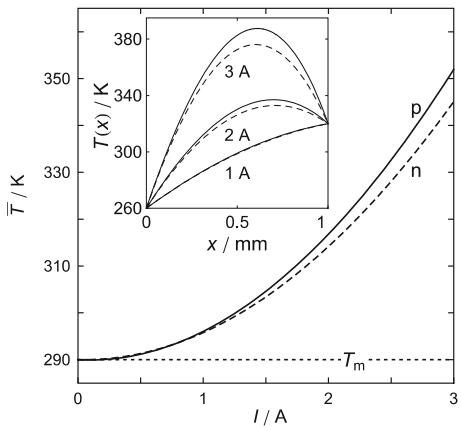

Fig. 3. For electric currents of practical interest in TEC, the average $\bar{T}$ of the temperature distribution along each leg (inset) is much larger than $T_m = (T_c + T_h)/2$. For the low currents $I < 0.4$ A used in TEG, the difference $\bar{T} - T_m$ is below 2% of $\Delta T = T_h - T_c$.

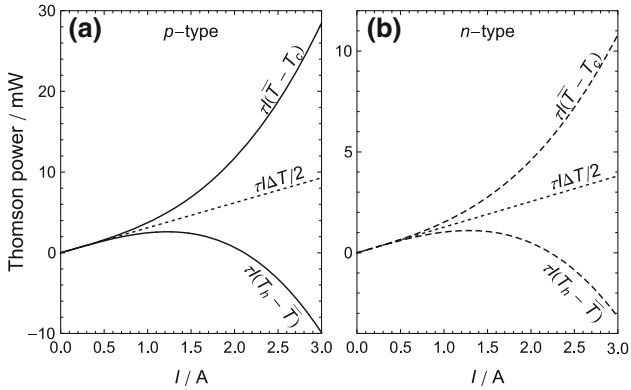

Fig. 4. Thomson contributions to the heat flows at the boundaries of the p-type (a) and n-type (b) legs. In the standard CTC model, these contributions are estimated as $\tau I \Delta T/2$, which underestimates their importance at both sides and fails to predict the correct sign at the hot boundary. In the improved CTC model, they are $\tau I(\bar{T} - T_c)$ and $\tau I(T_h - \bar{T})$. While $T_h - T_m = \Delta T/2$ is always positive, $T_h - \bar{T}$ reverses sign and becomes negative for moderate and large currents.

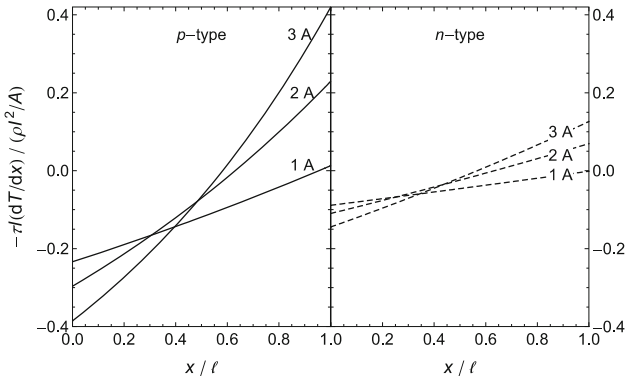

Fig. 5. Ratio of the local linear densities of Thomson power to Joule power in the *p*-type and *n*-type legs of a TEC for currents 1 A, 2 A and 3 A.

The comparison of the Thomson contributions to the heat flux estimated from the standard and improved CTC models evidences important discrepancies for TEC applications (Fig. 4). For a current of 3.0 A, the standard CTC model predicts a value three times smaller than the improved model. The standard CTC model underestimates the importance of the Thomson components at both boundaries. More importantly, it fails in predicting the correct sign because $T_h - T_m = \Delta T/2$ is always positive but $T_h - \bar{T}$ reverses sign and becomes negative for moderate and large currents. Therefore, the heat flows at the TE boundaries are more accurately described by Eqs. 6 and 7 than by Eqs. 3 and 4. These comments are of interest when the TEM operates in TEC mode, where the current can reach 3.0 A (Fig. 2a). However, for the smaller currents used in TEG mode (Fig. 2b), the standard CTC model is accurate enough.

The Thomson effect enhances the thermoelectric cooling at the cold junction of a TEM because the Thomson term $\tau I(\bar{T} - T_c)$ in Eq. 6 is positive. Remarkably, since $\bar{T}$ can be much larger than T_m, the enhancement can be much larger than predicted by the standard CTC model, which uses $\tau I(T_m - T_c)$ in Eq. 3. The linear density of power $I^2\rho/A - \tau I(dT/dx)$ locally released by the current has two components with different spatial distributions. The Joule component has a uniform distribution along the TE. The Thomson component has a nonuniform distribution because of the nonlinear temperature distribution (Fig. 3). Remarkably, the Thomson component reverses its sign for currents above 1.0 A. Note that a negative value of $-\tau I(dT/dx)$ means that the current "absorbs" energy due to the Thomson effect. Negative values of the ratio $-\tau I(dT/dx)/(I^2\rho/A)$ indicate partial elimination of the dissipated Joule power by the Thomson effect (Fig. 5). The thermoelectric cooling is enhanced by the Thomson effect: a current $I = 3.0$ A absorbs close to the cold side about 17% of the Joule power in the *n*-type leg and about 40% in the *p*-type leg.

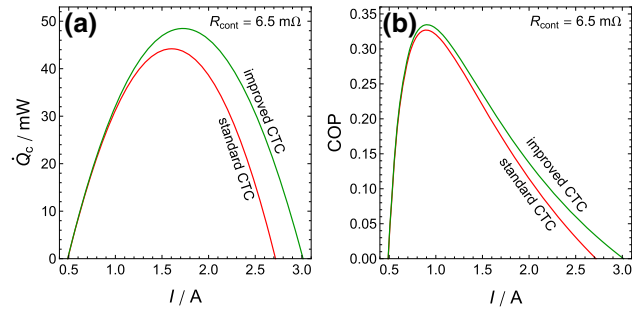

Fig. 6. The standard CTC model predicts a significantly lower cooling capacity (a) and a lower COP (b) than the improved CTC model. A contact resistance of 6.5 mΩ has been considered in these calculations.

Note, finally, that the inaccuracy in the estimation of the Thomson contributions implies that the standard CTC model predicts a significantly lower cooling capacity and a lower COP of the TEC than the improved CTC model (Fig. 6).

CONCLUSIONS

The CTC model (i.e., the approximation of replacing, in the local energy balance equation, the thermal conductivity, the electrical resistivity and the Thomson coefficient τ by constant values) has been reviewed. In its standard version, the power $\dot{W} = I^2R - \tau I\Delta T$ released by the current in the volume of the TE under steady-state conditions is further assumed to leave half through the cold boundary and the other half through the hot boundary.[7–16,18] Such an assumption can be only used for the low currents involved in TEG. In TEC applications, the fact that a larger fraction of this power leaves the TE through the hot boundary has significant implications. In particular, we have shown that the contributions of the Thomson powers are not $\tau I\Delta T/2$ and $-\tau I\Delta T/2$ but $\tau I(\bar{T} - T_c)$ and $-\tau I(T_h - \bar{T})$, where $\bar{T} = (1/\ell)\int_0^\ell T dx$ is the average temperature in the TE. In a TEC, the differences between these expressions are very relevant because the temperature distribution is nonlinear and the average temperature can be significantly different from the mean temperature of the hot and cold sides. We have analytically evaluated these Thomson powers in *n*-type $Bi_2(Te_{0.94}Se_{0.06})_3$ and *p*-type $(Bi_{0.25}Sb_{0.75})_2Te_3$ and shown that the simplified expressions, $\pm \tau I\Delta T/2$, used in the literature underestimate this contribution in up to a factor 3 and can even predict wrongly its sign at the hot side.

The improvement of the CTC model here described is important because, by describing more accurately the Thomson power contributions, it also leads to more accurate estimations of the cooling capacity and the COP of TEC.

ACKNOWLEDGMENTS

This work was supported by the Ministerio de Ciencia, Innovación y Universidades and European

Regional Development Funds through (project PGC2018-097359-B-100).

APPENDIX

The transport equations of thermoelectricity can be presented in the observable formulation as[22–26]

$$\mathbf{J}_E = -\kappa\nabla T + (\Pi - \mu/e)\boldsymbol{j} \tag{A1}$$

$$\nabla\mu/e = S\nabla T + \rho\boldsymbol{j}, \tag{A2}$$

where $\mathbf{J}_E$ is the energy flux density, μ is the electrochemical potential of the electrons and $e>0$ is the elementary charge. Different choices of flux densities and driving forces have been reviewed in Ref. 27. Under steady-state conditions, the local formulation of the energy conservation is $\nabla\cdot\mathbf{J}_E = 0$ or $\nabla\cdot(-\kappa\nabla T) - \rho j^2 + \tau\boldsymbol{j}\cdot\nabla T = 0$. The equivalent integral formulation states that no net energy leaves any volume V of the TE, $\oiint_\Sigma \mathbf{J}_E\cdot d\boldsymbol{A} = 0$, where Σ is the surface enclosing V. From Eq. A1, $\oiint_\Sigma \mathbf{J}_E\cdot d\boldsymbol{A} = 0$ can be decomposed in the energy that leaves V transported by thermal conduction, $\oiint_\Sigma(-\kappa\nabla T)\cdot d\mathbf{A} = \iiint_V \nabla\cdot(-\kappa\nabla T)dV$, and that transported by the current, $\oiint_\Sigma(\Pi - \mu/e)\boldsymbol{j}\cdot\ d\boldsymbol{A} = \iiint_V(\tau\boldsymbol{j}\ \cdot\nabla T - \rho j^2)dV$, where charge conservation $\nabla\cdot\boldsymbol{j} = 0$ has been used.

REFERENCES

1. W.H. Chen, C.Y. Liao, and C.I. Hung, *Appl. Energy* 89, 464 (2012). https://doi.org/10.1016/j.apenergy.2011.08.022.
2. H.S. Lee, *Energy* 56, 61 (2013). https://doi.org/10.1016/j.energy.2013.04.049.
3. A. Martínez, D. Astrain, A. Rodríguez, and P. Aranguren, *Appl. Thermal Engn.* 95, 339 (2016). https://doi.org/10.1016/j.applthermaleng.2015.11.021.
4. X.D. Wang, Y.X. Huang, C.H. Cheng, and D.T.W. Lin, *Energy* 47, 488 (2012). https://doi.org/10.1016/j.energy.2012.09.019.
5. E. Kanimba, M. Pearson, J. Sharp, D. Stokes, and S. Priya, *Energy* 142, 813 (2018). https://doi.org/10.1016/j.energy.2017.10.067.
6. J.H. Meng, X.D. Wang, and X.X. Zhang, *Appl. Energy* 108, 340 (2013). https://doi.org/10.1016/j.apenergy.2013.03.051.
7. S.C. Kaushik and S. Manikandan, *Cryogenics* 72, 57 (2015). https://doi.org/10.1016/j.cryogenics.2015.08.004.
8. S. Manikandan and S.C. Kaushik, *Energy* 100, 227 (2016). https://doi.org/10.1016/j.energy.2016.01.092.
9. P.E. Ruiz-Ortega and M.A. Olivares-Robles, *Entropy* 19, 312 (2017). https://doi.org/10.3390/e19070312.
10. G. Fraisse, J. Ramousse, D. Sgorlon, and C. Goupil, *Energy Convers. Manag.* 65, 351 (2013). https://doi.org/10.1016/j.enconman.2012.08.022.
11. G. Fraisse, M. Lazard, C. Goupil, and J.Y. Serrat, *Int. J. Heat Mass Transf.* 53, 3503 (2010). https://doi.org/10.1016/j.ijheatmasstransfer.2010.04.011.
12. G. Min, D.M. Rowe, and K. Kontostavlakis, *J. Phys. D Appl. Phys.* 37, 1301 (2004). https://doi.org/10.1088/0022-3727/37/8/020.
13. R. Arora and R. Arora, *Int. J. Energy Res.* 42, 1760 (2018). https://doi.org/10.1002/er.3988.
14. Y. Feng, L. Chen, F. Meng, and F. Sun, *Entropy* 20, 29 (2018). https://doi.org/10.3390/e20010029.
15. D. Zhao and G. Tan, *Appl. Therm. Eng.* 66, 15 (2014). https://doi.org/10.1016/j.applthermaleng.2014.01.074.
16. F. Meng, L. Chen, and F. Sun, *Energy* 36, 3513 (2011). https://doi.org/10.1016/j.energy.2011.03.057.
17. K. Zabrocki, C. Goupil, H. Ouerdane, Y. Apertet, W. Seifert, and E. Müller in, *Continuum Theory and Modeling of Thermoelectric Elements*, ed. by C. Goupil (Weinheim: Wiley-VCH, 2016), pp. 75–156, https://doi.org/10.1002/9783527338405.ch2.
18. A.F. Ioffe, *Semiconductor Thermoelements and Thermoelectric Cooling* (London: Infosearch, 1957).
19. H.S. Kim, W. Liu, and Z. Ren, *J. Appl. Phys.* 118, 115103 (2015). https://doi.org/10.1063/1.4930869.
20. J. Chen and Z. Yan, *J. Appl. Phys.* 79, 8823 (1996). https://doi.org/10.1063/1.362507.
21. A. Chakraborty, B.B. Saha, S. Koyama, and K.C. Ng, *Int. J. Heat Mass Transf.* 49, 3547 (2006). https://doi.org/10.1016/j.ijheatmasstransfer.2006.02.047.
22. J. Garrido, *J. Phys.: Condens. Matter* 21, 155802 (2009). https://doi.org/10.1088/0953-8984/21/15/155802.
23. J. Garrido and A. Casanovas, *J. Appl. Phys.* 115, 123517 (2014). https://doi.org/10.1063/1.4869776.
24. J. Garrido, *J. Phys. Chem. B* 106, 10722 (2002). https://doi.org/10.1021/jp020196k.
25. J. Garrido, *J. Phys. Chem. B* 108, 18336 (2004). https://doi.org/10.1021/jp049264o.
26. J. Garrido and A. Casanovas, *J. Electron. Mater.* 41, 1990 (2012). https://doi.org/10.1007/s11664-012-1966-0.
27. J.A. Manzanares, M. Jokinen, and J. Cervera, *J. Non-Equilib. Thermodyn.* 40, 211 (2015). https://doi.org/10.1515/jnet-2015-0026.
28. J.L. Pérez-Aparicio, R. Palma, and R.L. Taylor, *Int. J. Heat Mass Transf.* 55, 1363 (2012). https://doi.org/10.1016/j.ijheatmasstransfer.2011.08.031.
29. B.L. Wang, *Appl. Thermal Eng.* 110, 136 (2017). https://doi.org/10.1016/j.applthermaleng.2016.08.115.
30. T. Zhang, *J. Electron. Mater.* 46, 14 (2017). https://doi.org/10.1007/s11664-016-4932-4.
31. X.C. Xuan, K.C. Ng, C. Yap, and H.T. Chua, *Int. J. Heat Mass Transf.* 45, 5159 (2017). https://doi.org/10.1016/S0017-9310(02)00217-X.
32. I. Lashkevych, J.E. Velázquez, O.Y. Titov, and Y.G. Gurevich, *J. Electron. Mater.* 47, 3189 (2018). https://doi.org/10.1007/s11664-018-6205-x.
33. C. Ju, G. Dui, H.H. Zheng, and L. Xin, *Energy* 124, 249 (2017). https://doi.org/10.1016/j.energy.2017.02.020.
34. Y. Apertet and C. Goupil, *Int. J. Thermal Sci.* 104, 225 (2016). https://doi.org/10.1016/j.ijthermalsci.2016.01.009.
35. C.A. Badillo-Ruiz, M.A. Olivares-Robles, and P.E. Ruiz-Ortega, *Entropy* 20, 118 (2018). https://doi.org/10.3390/e20020118.
36. Y. Ge, Z. Liu, H. Sun, and W. Liu, *Energy* 147, 1060 (2018). https://doi.org/10.1016/j.energy.2018.01.099.
37. O. Yamashita, *J. Mater. Sci.* 40, 6439 (2005). https://doi.org/10.1007/s10853-005-1712-6.
38. D. Ebling, K. Bartholomé, M. Bartel, and M. Jägle, *J. Electron. Mat.* 39, 1376 (2010). https://doi.org/10.1007/s11664-010-1331-0.
39. H.J. Goldsmid, *Electronic Refrigeration* (London: Pion, 1986).